

THE EFFECTS OF FIRE ON ROCK ART: MICROSCOPIC EVIDENCE
REVEALS THE IMPORTANCE OF WEATHERING RINDS

Alice M. Tratebas

**Bureau of Land Management
1101 Washington Boulevard
Newcastle, Wyoming 82701**

Niccole Villa Cervený

**Cultural Sciences Department
Mesa Community College
7110 East McKellips Road
Mesa, Arizona 85207**

Ronald I. Dorn

**Department of Geography
Arizona State University
Tempe, Arizona 85287-0104**

Abstract: This paper presents results of the first study of pre-fire and post-fire samples collected from rock engravings and adjacent sandstone joint faces. A 2001 wildfire at Whoopup Canyon, Wyoming, stimulated a comparison of 1991 and 2003 samples. Optical microscopy of ultra-thin sections, backscattered electron microscopy, x-ray (energy dispersive and wavelength dispersive) analysis of cross sections, and high-resolution transmission electron microscopy reveal that fires create some thermal fractures that enhance panel erosion, but most of the fire-induced erosion occurs along weathering rinds that form long before petroglyph manufacturing. In addition, rock varnish on top of petroglyphs experiences spalling, and fire ash with a clear potassium spike strongly adheres to rock varnish on petroglyphs and spalled sandstone. In the past, site managers assumed minimal damage away from massive spalls and other macrodamage on fire affected petroglyphs, an assumption no longer tenable. Since it is difficult to protect rock art after a fire starts, mitigation efforts can include identification of areas of intense weathering-rind development as locales most susceptible to erosion, and clearing trees and shrubs near rock art by hand. [Key words: geomorphology, fire, rock art, sandstone, weathering.]

INTRODUCTION

Fire alters the appearance of landscapes in a dramatic fashion. Rock art panels are not excluded from fire damage (Kelly and McCarthy, 2001). Consider how fire changes soil formation and erosion processes (Morris and Moses, 1987; Prosser and Williams, 1998; Mazhitova, 2000) that then move fire-altered sediment over panels. Fire-induced episodic sediment erosion even modifies loci and timing of possible panel burial in downstream areas (Germanosky and Miller, 1995; Cerda, 1998).

A tremendous potential exists in rock art research to explore fire-altered deposits in and around panels using pedoanthracological methods (Carcaillet and Thion, 1996; Carcaillet, 1998; Harrison and Frink, 2000; Frink and Dorn, 2002). Maceral, sedimentological, organic geochemistry analyses of organic remains in soil, regolith, and nearby deposits also facilitate understanding of ancient fires (Siffedine et al., 1994; Lichtfouse et al., 1997; Lichtfouse, 1999; Laird and Campbell, 2000) in and around rock art sites. Many interfaces between physical geography, fire, and rock art research remain unresearched.

The specific aspect that we explore here rests in the study of weathering processes. Unfortunately for rock art researchers, the specialized literature on fire as a weathering process is in its infancy. Geomorphologists have long known of the importance of fire in rock weathering (Blackwelder, 1927), and rock-art researchers have begun to recognize the overall importance of fire (Kelly and McCarthy, 2001). However, the fire weathering literature suffers from a paucity of good data, since it consists primarily of semi-quantitative observations (Emery, 1944; Ollier, 1983; Dragovich, 1993). Consider the importance of burning epilithic organisms such as lichens that form on panels. Even though excellent review papers exist on biological weathering (Viles, 1995, 2001), only one paper examined the influence of fire on rock surface organisms or lithobionts (Garty, 1992). The state of field knowledge is so poor that quantitative observations on rates of fire-induced erosion are decades apart (Zimmerman et al., 1994; Dorn, 2003).

Archaeologists, ecologists, and experimental geomorphologists provide rock art researchers with the first glimpse of theory by which the potential impact of fire on rock art panels might be understood. Archaeologists contribute models of thermolithofractography as a means to characterize and interpret "fire cracked" rock (House and Smith, 1975; McFarland, 1977; Kritzer, 1995; Rapp et al., 1999; Wilson, 1999). Ecologists offer rock art research insight into changes in nutrient cycles such as potassium (Brais et al., 2000) used in cation-ratio dating (Pineda et al., 1990; Zhang et al., 1990; Whitley and Annegarn, 1994; Plakht et al., 2000). Geomorphologists provide insight from laboratory experiments on fire (Goudie et al., 1992; Allison and Goudie, 1994; Nealson, 1995; Allison and Bristow, 1999), elucidating that erosion of rocks after a fire depends heavily on rock physical properties, varies with different rock types, and increases with the water content of the rock. Geomorphologists also offer perspectives on the importance of prior "inherited" weathering on erosion processes (Pope, 2000; Pope et al., 2002; Gordon and Dorn, 2005).

Given the aforementioned general state of empirical knowledge and theory of how fires might impact rock art panels, we offer this first contribution on a wildfire's effect on rock art where pre-fire samples can be compared with post-fire collections. We believe that fire and its effects can be part of a productive dialogue among physical geographers, archaeologists, and site managers.

The traditional organization of a scientific paper separates methods from results and discussions. We disembark from that constraint, because we utilize a wide variety of methods to understand the change brought about by fire. We feel it is best if the reader is able to balance methodological limitations with findings, side-by-side,

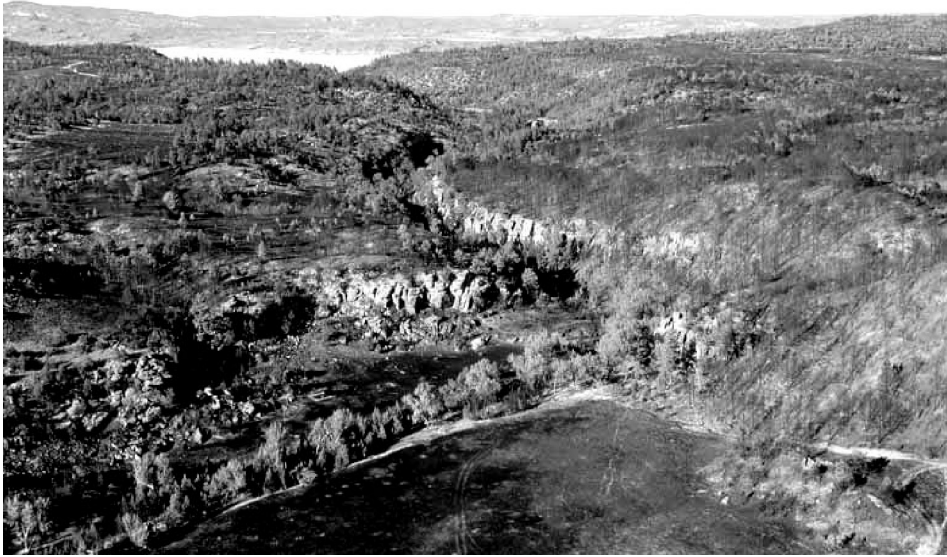


Fig. 1. Oblique helicopter photograph of Whoopup Canyon, Wyoming, after the fire. Sandstone joint faces on the canyon walls host petroglyph panels.

in the same section. We first start, however, with the traditional study site description, along with an explanation of our sample selection strategy.

STUDY SITE

A wildfire damaged the Whoopup Canyon petroglyph site in 2001. Petroglyphs extend along 9.6 km of a canyon that cuts through sandstone cuestas on the western flank of the Black Hills, Wyoming (Fig. 1). The fire was typical for the western Black Hills in initiation by lightning with a fast run across several miles of terrain in the first two days. Petroglyph panels in the narrow sections of the canyon escaped the burning of nearby fuels although trees on the rims and ridgetops above them burned. Petroglyphs on cliffs in wider openings of the canyon experienced a blasting fire storm. The south end of the site escaped the fire storm. Petroglyphs there, however, were affected by a back burn, that was allowed to move to within 6 m of the petroglyphs, despite instructions to keep flames at least 0.8 km.

The site has 150 petroglyph panels. Most are Early Hunting style pecked images that depict game animals, hunting scenes, and humans conducting ceremonies (Tratebas, 1993; Tratebas, 2000). Experimental dating in 1991 by cation-ratio and ^{14}C methods suggested that the petroglyphs spanned thousands of years, ranging back possibly to more than 11,000 yrs. The most severe fire damage was to the largest cluster of panels at the site. Almost half of the cation-ratio and radiocarbon

samples in the earlier research came from these panels. We believe it is fortunate that the panels were sampled and analyzed prior to the fire, rather than waiting a decade or two for rock-art dating methods to be refined, or we would not have obtained pre-fire insight into the nature of weathering at these panels. Macroscopic observations after the fire showed small scale spalling of petroglyphs and ash deposits that raised the issues of: whether the fire damaged the varnish and rock substrate in ways not visible to the eye, and whether ash and carbon deposits from the fire contaminated the glyphs for dating.

SAMPLE SELECTION

We used two strategies in post-fire sampling. One was to sample panels where damage was obvious—spalls, visible ash deposits, burned lichen next to motifs, and fire-reddened areas. Most of these panels rest in close proximity to burned trees, and data on distance to burned trees permits comparisons between fuels burned and observed petroglyph damage. The second strategy involved collecting samples from the same glyphs sampled in 1991. These paired pre- and post-fire samples enable us to examine the effect of the fire by the study of thin-sections and cross-sections of the rock coatings and the underlying rock.

We use here a numbering sequence of petroglyph panels and sample numbers. Petroglyph panels are sequential numbers assigned as panels are discovered. Adjacent panels are indicated by decimals. For example three adjacent panels might be 6.1, 6.2, and 6.3. Sample numbers have three parts: (1)WC designates the site, (2) 91 or 03 represents the year of collection, and (3) the last number is the sequential sample number.

INDUCTIVELY COUPLED PLASMA CHEMICAL ANALYSES

We wanted to understand the chemistry of the fine particulate matter that flowed as suspended load over panel faces after the fire. Thus, we sampled the latest flash-flood deposits from Whoopup Creek banked up against the base of Panel 17.1. The remainder of the samples included gray-white ash mixed with inorganic fines. We did not exclude any particular particle size from the analyses, but 95% of the oven dry weight of each sample contained fine sand and smaller particles.

Inductively-coupled plasma (ICP) atomic emission spectroscopy data reveal that the chemistry of the “fire ash” that flowed over panel faces (last three columns in Table 1) has a similar signature. The most notable result is high concentration of potassium (K) relative to other elements. K is highest in the ash-filled last stage flood deposit and is only slightly less common in overland-flow deposits draped over panel faces. This is in contrast with a much lower elemental abundance of K in the flash flood deposits that contain little ash.

Potassium is a key component of cation-ratio (CR) dating (Pineda et al., 1990; Zhang et al., 1990; Whitley and Annegarn, 1994; Plakht et al., 2000), and potassium anomalies were seen in optical and electron micrographs discussed later. Since ICP is a “bulk” chemical analysis technique, ICP data strongly suggest that the place-specific microscope observations reflect a general process operating after the

Table 1. Inductively Coupled Plasma Atomic-Emission Spectroscopy Elemental Analyses of Sediments Deposited on Tops of Panels and Petroglyphs^a

Sediment	Panel number, sample identification number, and sample				
	17.1	17.1	52.1	20.2	20.1
	WC-03-28	WC-03-28	WC-03-27	WC-03-08	WC-03-05
	Early flood stage	Last flood stage	Panel face	Panel face	Ash in pockets on slender-leg deer
K %	1.50	6.47	4.59	4.21	4.67
Al %	3.34	1.15	3.49	3.38	3.80
Ca %	5.32	0.56	5.52	5.90	5.37
Fe %	1.54	0.85	1.56	1.01	1.64
Mg %	1.08	0.16	1.13	0.86	1.20
Na %	0.33	0.12	0.35	0.24	0.37
S %	0.10	0.07	0.11	0.03	0.14
Ti %	0.19	0.09	0.19	0.13	0.21
Ag ppm ^b	0.08	0.07	0.07	0.06	0.09
As ppm	6.10	4.80	5.80	4.10	5.80
Ba ppm	360.00	170.00	370.00	280.00	400.00
Be ppm	0.90	0.35	0.81	0.63	0.93
Bi ppm	0.20	0.11	0.19	0.09	0.21
Cd ppm	0.41	0.19	0.43	0.23	0.48
Ce ppm	42.30	25.40	42.00	29.90	43.40
Co ppm	5.70	2.80	5.60	3.90	5.80
Cr ppm	152.00	228.00	126.00	74.00	130.00
Cs ppm	2.80	0.97	2.80	1.86	3.09
Cu ppm	14.00	7.40	13.00	8.50	13.20
Ga ppm	7.21	2.77	7.21	4.97	7.72
Ge ppm	0.24	0.13	0.24	0.18	0.23
Hf ppm	0.10	0.10	0.10	0.10	0.10
In ppm	0.02	0.01	0.02	0.01	0.02
La ppm	21.70	12.10	22.40	14.90	22.50
Li ppm	18.80	8.60	19.40	13.70	20.30
Mn ppm	353.00	136.00	365.00	239.00	399.00
Mo ppm	2.68	1.14	2.22	1.44	2.71
Nb ppm	3.60	1.60	3.50	2.20	3.70
Ni ppm	17.60	11.60	15.20	11.10	17.10
P ppm	450.00	260.00	480.00	280.00	540.00
Pb ppm	14.80	13.10	14.90	8.10	16.80
Rb ppm	49.20	17.00	50.60	35.40	52.80
Sb ppm	0.38	0.27	0.39	0.24	0.40

(table continues)

Table 1. (Continued)

Sediment	Panel number, sample identification number, and sample				
	17.1	17.1	52.1	20.2	20.1
	WC-03-28	WC-03-28	WC-03-27	WC-03-08	WC-03-05
	Early flood stage	Last flood stage	Panel face	Panel face	Ash in pockets on slender-leg deer
Se ppm	1.00	1.00	1.00	1.00	2.00
Sn ppm	0.90	0.60	0.90	0.50	1.00
Sr ppm	161.00	358.60	367.00	327.50	377.00
Th ppm	6.80	3.00	6.60	4.30	7.00
Tl ppm	0.35	0.13	0.31	0.22	0.36
U ppm	2.00	0.90	1.90	1.50	2.00
V ppm	45.00	16.00	46.00	30.00	50.00
W ppm	0.70	0.40	0.50	0.40	0.60
Y ppm	10.40	4.80	10.30	7.50	10.80
Zn ppm	45.00	24.00	45.00	24.00	50.00
Zr ppm	4.20	3.00	4.20	2.60	5.90

^aSediment that was draped over panels as a result of the fire greatly increased the abundance of potassium.

^bPpm refers to parts per million.

fire. Our preliminary conclusion is that the fire ash probably has a high concentration of potassium, and that the fire ash does appear to pose a complication to future attempts at dating petroglyphs by the cation-ratio method.

OPTICAL MICROSCOPY

Overview

Light microscopy of ultra-thin sections allowed us to see the bigger “microscopic picture” before delving into higher magnification electron microscope methods. The technique is simple in description and very difficult to carry out in the laboratory. Small chips are mounted in epoxy where the surface of the rock is “normal” to the cross-sectional surface. The chip is polished until it is possible to see through rock varnish. Since rock varnish is usually opaque in typical geological thin sections, the polishing process ends up being an art form where just a little too much abrasion erodes the cross section away while too little abrasion leaves the varnish completely opaque. This is the same technique used to see layering patterns within varnish (Dorn, 1992; Dorn, 2000; Liu, 2003).

Four general observations stand out. First, fire ash appears to adhere to panel faces, even though the ash is not visible to the observer in the field. Second, chalk applied to petroglyphs by uninformed visitors survived thermal stresses of the fire. Third, internal structures within rock varnish provided surfaces of fire spalling, and

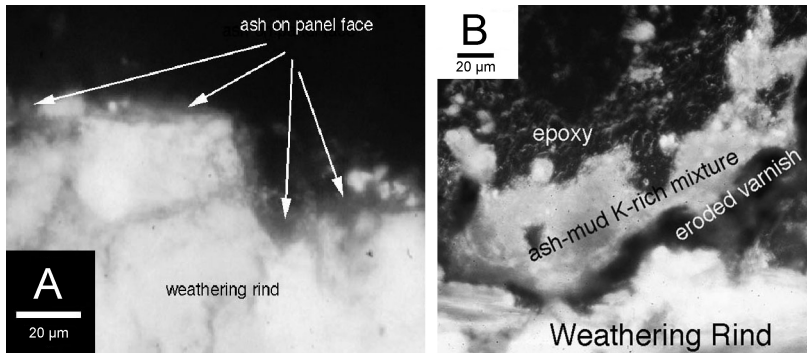


Fig. 2. Optical thin-section view of ash adherence to spalled surfaces. (A) Sample WC-03-43 derives from Panel 3.1, a fire spall where the pre-existing weathering rind formed the detachment surface. The ash survived two yrs. on the panel face by mixing with fragments of weathered quartz. The granular appearance of the quartz can be seen *in situ* within intact weathering rinds. (B) Sample WC-03-06 is from Human With Staff petroglyph. The pre-fire varnish was much thicker with a complete microlamination sequence, but the fire spalled most of the varnish. The varnish detached in zones of porosity weakened by cation leaching. Then, post-fire soil erosion washed sediment over the petroglyph, and a mixture of potassium-rich ash and inorganic sediment now adsorbs onto the eroded-varnish surface.

the apparent weakness comes from porous zones of cation leaching; thus, it is ironic that the very process that permits cation-ratio dating opened up a weakness to spall varnish and prevents the applicability of future dating in places of varnish erosion. Fourth, the fire appears to have generated fractures in the underlying rock that might accelerate future erosion of panels.

Ash Adherence

Ash adheres to joint faces newly exposed by fire (Fig. 2A). Ash also attaches to petroglyphs (Fig. 2B). These ultra-thin sections exemplify several potential consequences of the fire to petroglyphs. Ash adherence appears to be fairly firm in that the extant ash adsorbs to porous surfaces. The porous surfaces inside rock varnish are sites of cation-leaching (Dorn and Krinsley, 1991). When we put these thin sections in an electron microscope column, energy-dispersive x-ray analyses reveal that the ash had a strong potassium signal, consistent with ICP measurements of the ash discussed in a later section. Since K is an important part of cation-ratio (CR) dating, the presence of ash prevents use by this calibrated dating method.

In addition to the presence of adsorbed ash, Fig. 2B demonstrates that spalling of the panel took place within previously weathered rinds. Large fresh quartz grains that would be produced by thermal fracturing are not in evidence; rather, the chaotic and irregularly-shaped fragments of quartz indicate that the ash may be preserved by mixing with the pre-existing weathering rind fragments.

The source of the ash could have derived from two sources. The fire storm itself may have blasted ash onto surfaces, accounting for the strong adherence. Alternatively, ash settling onto surfaces above the panel may have been transported later

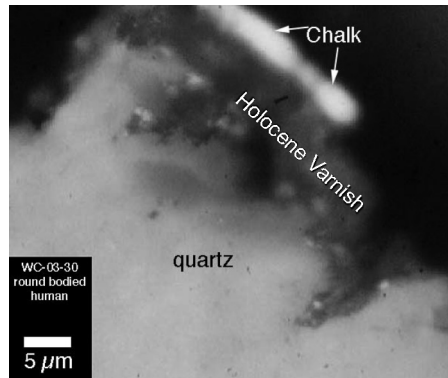


Fig. 3. Optical thin section image of chalk applied to petroglyph surfaces survived the fire. Sample WC-03-30, from a Round-Bodied Human petroglyph, reveals that chalk adhered to the surface of the varnish so strongly that it took erosion of the entire sequence of rock and varnish to remove this foreign material. According to Liu's (2003) calibration, this section displays a Holocene (only orange-yellow) varnish microlamination sequence.

over rock faces from overland flow. We cannot discern from these analyses whether a firestorm or overland flow source is more likely.

Chalking Survives Fire

Samples collected prior to the fire revealed a strong chalking signal, both in electron microscope observations and in chemical analyses undertaken for CR dating. We anticipated that the thermal effects of the fire might have dislodged chalk applied to petroglyphs by uneducated prior observers. However, we encountered enough chalk in the post-fire thin sections (e.g., Fig. 3) to reveal the legacy of those attempting to improve their photographs. The identification of chalk in these optical sections was confirmed by energy dispersive x-ray analyses showing an overwhelmingly strong calcium spike.

Intravarnish Erosion

The fire appears to have increased the erosion of varnish. Sometimes, the erosion surface occurs within the varnish itself, as seen in Fig. 2B. At other times, the erosion surface appears to be within the weathering rind underneath the varnish, where only deep pockets of varnish survived (Fig. 4). In both circumstances, the net effect leaves behind pockets of partially preserved varnish. An incomplete varnish, of course, invalidates varnish chronometry.

Grain Fractures

In addition to erosion along previously weathered material, there is evidence of increased mechanical fracturing in minerals that did not erode as a consequence of

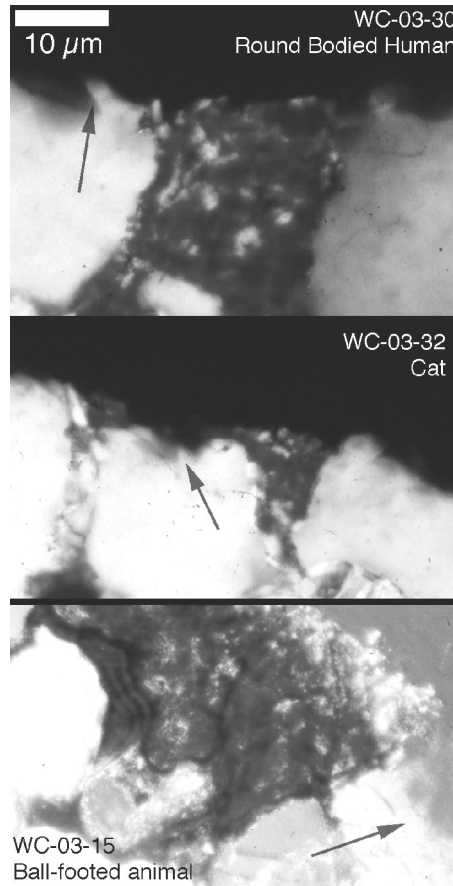


Fig. 4. The wildfire appears to have caused, in some cases, the varnish to separate from the underlying weathering rind. In these optical thin section examples, erosion of the pre-weathered rock resulted in a pattern where remnants of varnish exist only in tiny pockets. Arrows point to quartz that eroded on surfaces decayed over a long period of time, well before the fire event. Mechanical fire weathering, in contrast, generates much cleaner fractures (Dorn, 2003). The scale bar applies to all photomicrographs, where the petroglyph samples from top to bottom are WC-03-30 (Round Bodied Human), WC-03-32 (Cat), and WC-03-15 (Ball-Footed Animal).

the fire (Fig. 5). In counts of 30 quartz grains in pre-fire and post-fire samples, sub-parallel fractures inside the quartz increased in abundance from the pre-fire (1991) to the post-fire (2003) samples by a factor of about three. These cracks appear to be mechanical fractures, cutting across relatively unweathered and weathered grains. We speculate that fire-induced thermal fracturing might play a role in the development of weathering rinds. These fractures could increase surface area sufficiently to enhance the granular quartz weathering patterns seen in electron microscopy.

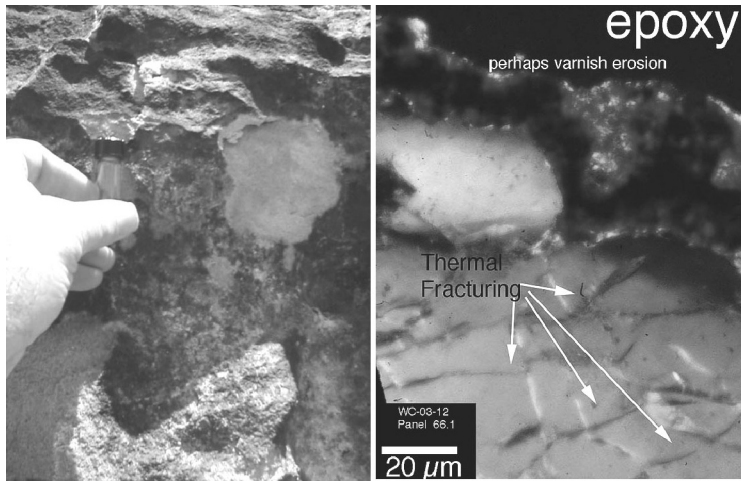


Fig. 5. Optical thin section sample WC-03-12 from a panel that acted like a fire chimney. Detachment surfaces are in the weathering rind. Two potential consequences of the fire can be seen. First, the host quartz appears to have undergone thermal fracturing. The linear fracturing, exemplified by the arrows, appears to cut across both relatively fresh and more weathered grains. Certainly, we saw grain fractures in the 1991 pre-fire samples. However, the abundance of these subparallel fractures appears to have increased dramatically. Second, rock varnish on the panel appears to have experienced spalling.

ELECTRON MICROSCOPY

We used several electron microscope methods. High resolution transmission electron microscopy (HRTEM) facilitated an analysis of weathering of the quartz at very high magnifications, while scanning electron microscopy (SEM) allowed us to examine fire erosion at magnifications between optical and HRTEM. We used two different types of SEM detectors. Backscattered electron microscopy (BSE) images the chemistry of the cross section by allowing us to see average atomic number and porosity (Dorn, 1995), while secondary electron microscopy (SE) allows us to image the topography of these same sections. *In situ* chemical analysis by energy-dispersive and wavelength-dispersive analysis of X-rays (Reed, 1993) provided supplemental information.

High-Resolution Transmission Electron Microscopy

An important issue is whether the fire altered the fundamental structure of the host quartz mineral grains. This is different from the creation of the mechanical fractures. The question asked in this section is whether the quartz grains were altered at a mineralogical level. HRTEM has been used successfully, for example, to understand natural quartz decrystallization (Pope, 1995) as part of a smaller-scale process of quartz weathering. HRTEM has also been used to understand the layering structure and biological signals in rock varnish (Krinsley et al., 1995).

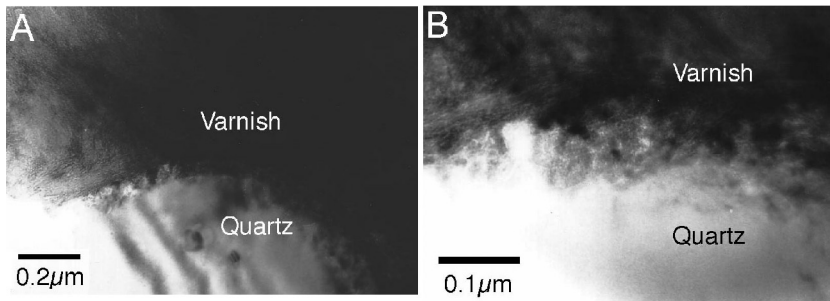


Fig. 6. Comparison of (A) 1991 pre-fire and (B) 2003 post-fire samples of a “hobbled deer” petroglyph (pre-fire sample WC-91-16 at panel 24.1; post-fire sample WC-03-16). The same types of crystal defects and decrystallization occur in pre-fire and post-fire imagery. These HRTEM views also illustrate that Whoopup varnish starts to form on quartz surfaces with an irregular topography—helping in varnish nucleation (Dorn, 1988).

We examined two pairs of pre-fire and post-fire samples, a loopline petroglyph (pre-fire sample WC-91-2 at panel 20.2; post-fire sample WC-03-09) and a hobbled deer petroglyph (pre-fire sample WC-91-16 at panel 24.1; post-fire sample WC-03-16). In each case, the focus rests with quartz grains at the very top of the petroglyph surface where we used the varnish to orient ourselves.

Based on this limited sample set, the Whoopup fire did not appear to alter the basic nature of the quartz grains. Careful qualitative examination of the HRTEM imagery failed to reveal clear mineralogical changes (e.g., Fig. 6). We found the same basic defects in pre-fire and post-fire samples.

It is important, however, to understand a limitation of this method. HRTEM does not reveal chemical insights, but only structural information. Chemical changes could have taken place and would not be discernible through this approach. Still, HRTEM is a difficult and very time-consuming method in terms of sample preparation and can yield important mineralogical insights at very high spatial resolution.

Backscattered Electron Microscopy

BSE imagery provides the greatest insight into processes by which panels and petroglyphs survive or erode. Case hardening is the key agent of preservation, while the development of porous weathering rinds underneath the case hardening is the key agent of erosion.

Four main types of case-hardening agents help preserve panels and petroglyphs: (1) silica glaze (Dorn, 1998) cementation of the quartz grains; (2) a mixture of silica glaze and rock varnish acting as the cementing agent; (3) iron films with minimal porosity bind quartz grains together; and (4) rock coatings (Dorn, 1998) of iron films, rock varnish and oxalate crusts also act as a case-hardening agent, not by strengthening the host rock—but through the action of being a strong enough rock coating to inhibit detachment of quartz grains.

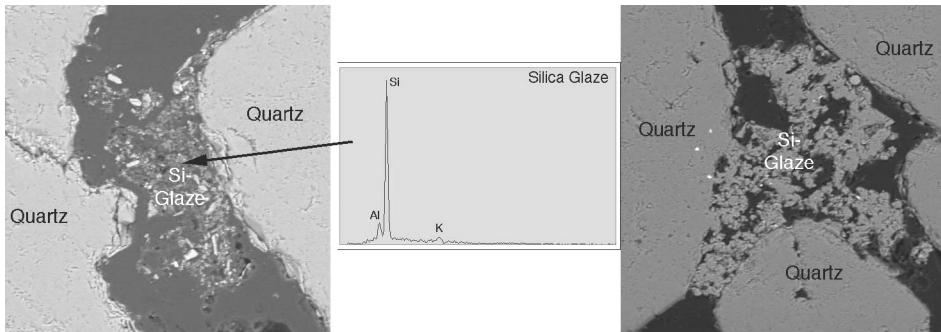


Fig. 7. This panel (20.2) BSE sample WC-03-11 came from an unexposed joint face, approximately 40 cm up into a joint still covered by an overlying block of sandstone. The sample displays the weakest of the case-hardening cements, a relatively porous silica glaze. Composed of mostly silicon, with minor amounts of aluminum and potassium, this silica glaze is typical of coatings found on the walls of sandstone joint faces at Whoopup. This “inherited” silica glaze displays two textures, disoriented platelets (left) and granular forms (right). Left image is 210 µm across and the right is 260 µm across.

Silica glaze (Dorn, 1998) is the weakest case-hardening agent, but it is porous enough to permit capillary water to flow in and out of a panel face. Silica glaze originally forms along the surfaces on joint planes (cf. Pentecost, 1991) prior to exposure as a panel face (Fig. 7). When the overlying sandstone spalls into talus, the “inherited” case hardening helps preserve joints long enough for stronger case-hardening agents to accumulate.

A slightly stronger case-hardening agent occurs where rock varnish cations are leached from the subaerial coating (Dorn and Krinsley, 1991) and reprecipitate within the underlying silica glaze. A mixture of silica glaze and rock varnish forms this most common type of case-hardening cementing agent (Fig. 8).

Iron films (Figs. 9 and 10) are the strongest type of case-hardening agent at Whoopup. These iron films most commonly occur in a stratigraphic sequence underneath subaerial rock varnish and also underneath a subsurface mixture of varnish redeposition and silica glaze (Fig. 9). However, iron films can sometimes occur at or close to the panel surface (Fig. 10).

The iron films seen at Whoopup are very similar to those observed at Karkevagge in the Arctic (Dixon et al., 2002; Thorn et al., 2001), requiring abundant acidity to mobilize the iron and silica. Iron precipitation can occur abiotically or with the aid of iron-oxidizing bacteria. We speculate that the abundant silica, from quartz dissolution, mixes with iron to form this case-hardening agent.

Iron films, however, can also act to accelerate panel erosion in two ways. First, the iron films mechanically fracture quartz grains. Comparable to Karkevagge in the Arctic (Dixon et al., 2002; Thorn et al., 2001), Figs. 10D, 10E, and 10F display mechanical fracturing of quartz grains by the precipitating iron films. This physical weathering is similar to “salt weathering” where chloride and carbonate precipitation fractures rock. Iron fracturing of quartz grains occurs in other settings in the Black Hills where intermittent water flow contains acidic discharges. As long as the

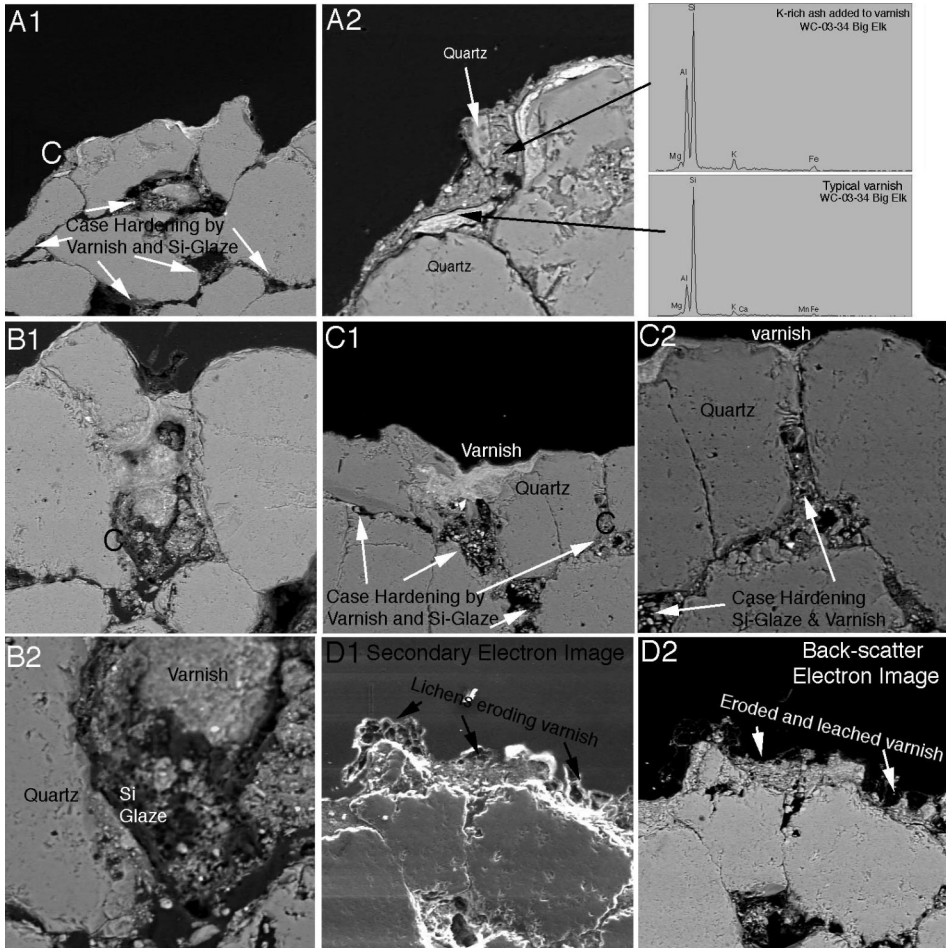


Fig. 8. These BSE images from a Big Elk Petroglyph (WC-03-34, WC-91-38, Panel 6.2) focus on case hardening by a mixture of silica glaze and rock varnish. Images A1, B1/B2, and C1/C2 all show case hardening of the petroglyph's quartz by a mix of silica glaze and rock varnish, where the silica could be "inherited" from subsurface cementation (Fig. 7). Rock varnish would then be added after the panel face is exposed by spalling. Images A2 and D1/D2 illustrate how the fire and microenvironment complicates varnish dating of petroglyphs. Image A2 displays a covering of clays and ash adhered reasonably well to the varnish. This ash covering contains a spike in potassium (K). The topographic (secondary) image D1 highlights the presence of lichens growing on top of the varnish. The chemical (backscatter) D2 image shows erosion and enhanced cation leaching of the rock varnish resulting in a much lower cation ratio than varnishes not influenced by lichens. Image widths: A1 (600 μm); A2 (140 μm); B1 (560 μm); B2 (180 μm); C1 (360 μm); C2 (110 μm); D1 (330 μm); D2 (330 μm). Image A2 is a close-up of the letter "C" in image A1.

iron films do not remobilize from an acidic event, the physical fracturing of the quartz would remain frozen glued together by the iron films. However, if the iron were to remobilize, a very porous weathering rind would result.

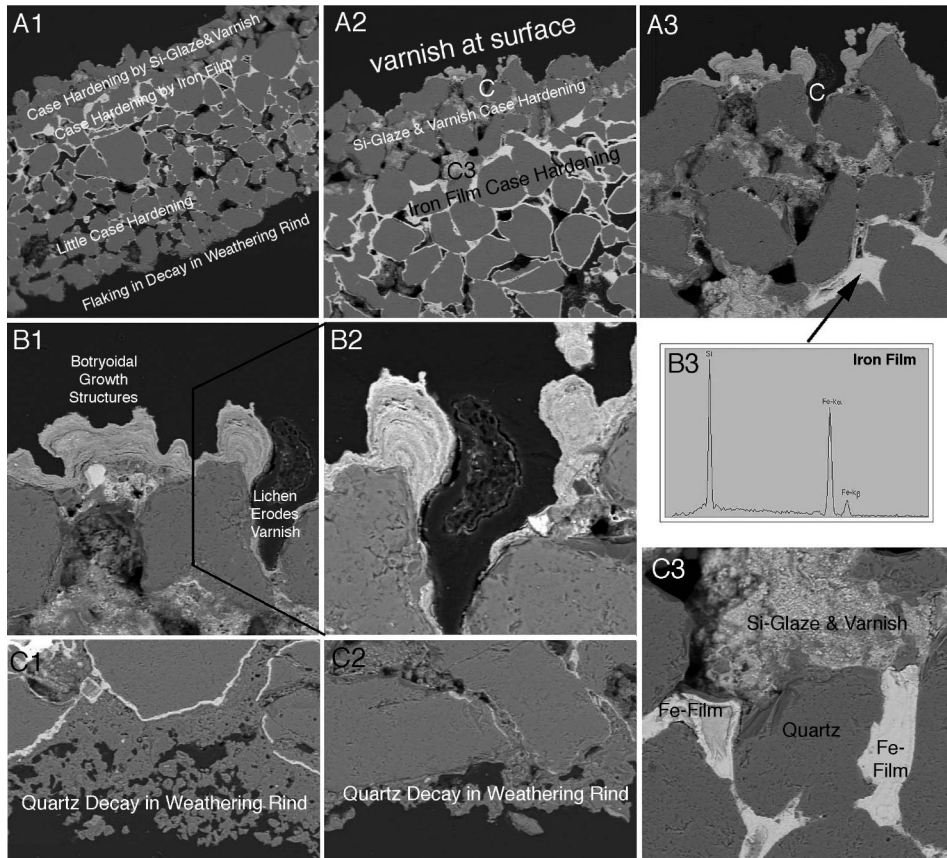


Fig. 9. BSE samples from the Human petroglyph (Panel 30.1, WC-03-49m, WC-91-38), exemplify case-hardening by iron films. Image A1 displays the full stratigraphy from top to bottom of: surficial layer of rock varnish; case hardening by a mixture of silica glaze and rock varnish; case hardening by iron film (a water-flow deposit containing silicon and iron); and a weathering rind underneath the iron film characterized by decayed quartz. Images A2 and A3 show progressive close-ups of the top three layers. Note the greater porosity of the varnish/Si-glaze case-hardening cement, compared with the iron film. Also note how the iron film is thickest towards the top and thins progressively further away from the panel surface. Image C3 presents the reasonably-distinct contact between these two case-hardening zones. Images C1 and C2 present the prevalent condition at the base of the samples: thorough decay of the quartz minerals. The quartz grains appear to be dissolving and undergoing granular decay. Such a condition could occur if acidic, iron-rich waters were dammed behind the iron film. Image B2 (and the lower magnification B1) illustrates a relatively common correlation: where lichens appear, the varnish appears to be completely eroded or in a state of erosion. The acid released by lichens dissolves the manganese and iron “glue” that holds the varnish together—resulting in the loss of varnish. The source of the iron could derive, in part, from lichen-generated acidity. Image widths: A1 (2200 μm); A2 (1400 μm); A3 (530 μm); B1 (240 μm); B2 (150 μm); C1 (250 μm); C2 (200 μm); C3 (600 μm).

A second way that iron films accelerate panel erosion is more problematic. The iron films are far less porous than case hardening by the mixture of varnish/Si-glaze. This means that water inside the sandstone would remain in the pores, just behind

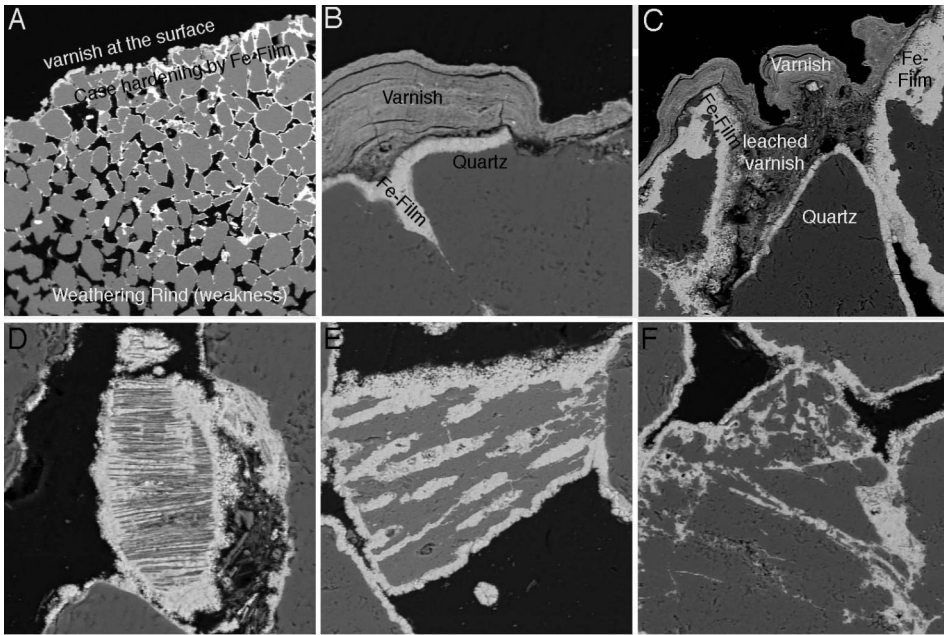


Fig. 10. These BSE images from a Dog petroglyph (Panel 6.2, WC-03-37, WC-91-39) illustrate where case hardening by iron films is right next to the surface. Images A, B, and C show iron film, alone, case hardening the sandstone. The varnish/Si-glaze case hardening appears to be missing, perhaps pecked away during petroglyph manufacturing. The rock varnish can be seen accreting directly on top of the iron film in images B and C. The iron film is thickest at the top and thins into micron threads at a depth of a few millimeters. Images D, E, and F display mechanical fracturing of the quartz grains by the precipitating iron films. Image widths: A (2200 μm); B (110 μm); C (270 μm); D (100 μm); E (100 μm); F (110 μm).

the iron film, for long periods of time. Water can escape from the rock along capillaries in the pores occupied by varnish/Si-glaze cementing. The tighter iron seal means intrasandstone water is able to weather the quartz. The result could be responsible for the observed intense quartz weathering (Fig. 9C1, 9C2) creating a very weak weathering rind.

Fire-induced spalling occurs most commonly within the pre-existing weathering rind. In a sampling of 10 spall chips from a panel, we did not observe “clean fractures” on the underside of any of the spalls (Fig. 11), as would be expected by purely thermal weathering. While case hardening held the very surface of the fire-impacted panel in place, the future erosion surface was already in a state of decay—ready to spall when fire generated thermal stress. Any capillary water stored in the weathering rind, even after weeks of drought, would have contributed to the fire spalling, since we know that moisture present in the rock greatly increases rates of fire decay (Goudie et al., 1992; Dorn, 2003).

The weathering rind represents centuries to millennia of decay underneath the surficial rock coatings (Gordon and Dorn, 2005). Even though quartz is a mineral very resistant to chemical weathering, quartz decay and the weathering of other rock minerals is evident throughout the site. The decay took place underneath the

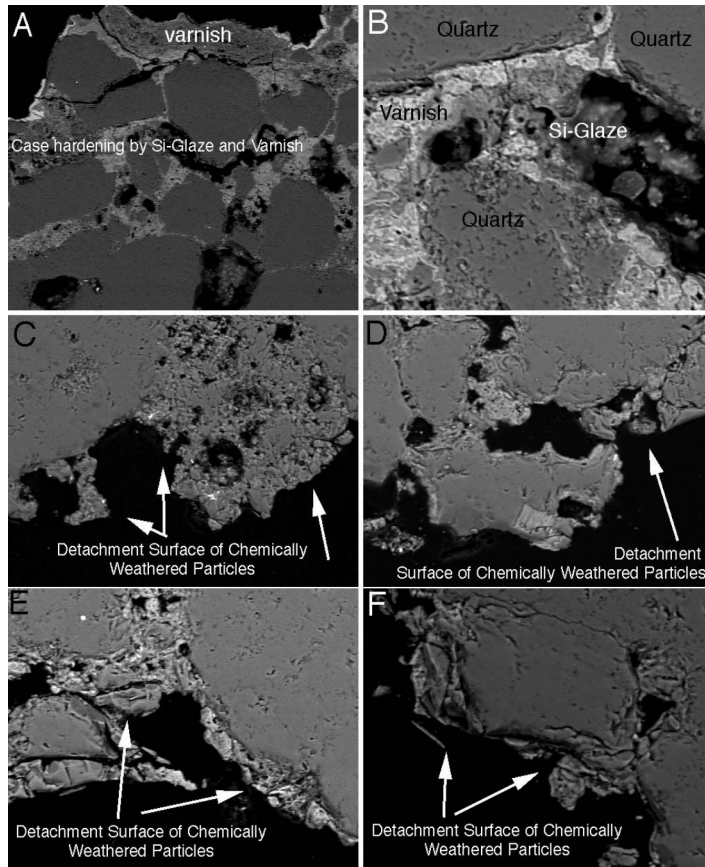


Fig. 11. From WC-03-43 (panel 3.1), these BSE images of spalled fragments illustrate the typical pattern of detachment in the weathering rind. Image A maintains a sequence of rock varnish underlain by quartz grains cemented by a combination of silica glaze and rock varnish. Image B presents a higher magnification view of the varnish/Si-glaze mixture case hardening the panel. Images C, D, E, and F display views of the underside of spalls; all detachments took place along chemically-weathered surfaces. Image widths: A (1800 μm); B (140 μm); C (180 μm); D (140 μm); E (150 μm); F (150 μm).

surficial rock coatings and mixtures of rock coating and rock material making a case hardening. Even under the mixture of varnish/Si-glaze case hardening, quartz grains decayed in the weathering rind. The decay is most extensive underneath the less porous iron film, and weathering has reached the point where failure occurs by disintegration of the weathered quartz. The fire spalls studied here appear to have failed extensively in this already-decayed weathering rind.

CONCLUDING THOUGHTS RELATED TO MANAGEMENT

This is the most complete study yet undertaken analyzing the effects of fire on petroglyphs. We are not aware of another study where pre-fire samples could be

compared with post-fire samples. As such, we have an obligation to present insights to those responsible for managing sites that could experience a wildfire. The reader should keep in mind, however, that our observations are based on analyses of only a few dozen samples in a particular lithologic and fire context. With these qualifications in mind, we make a number of management recommendations.

An important result of this research is that casual inspection is not sufficient for fire damage assessments. Considerable damage may be present, but cannot be seen with the eye. In consequence, site managers cannot assume that the rock art is unharmed if they do not see large scale spalls. In addition, managers should not assume that ash deposited in a fire will quickly erode away. Samples collected 2 yrs. after the fire had tightly adhering ash. This research also shows that fire damage to rock art occurs at much greater distances from burned trees than we would have guessed, particularly for ash deposits.

As a result, it is important to prevent wildfires from reaching rock art panels. It is important to avoid prescribed fires to reduce fuel loads where rock art is present. We do not know yet how much distance should be maintained between fires and rock art, because we have not conducted microscope analyses on enough fire-damaged rock art to draw reliable inferences on the distances between burned fuels and various kinds of fire damage. Certainly, wherever ash can settle out on rock art and soil surfaces that can wash onto rock art, damage from ash can be expected.

The severity of damage that is revealed by microscopy indicates that it is vital to cut trees and shrubs near rock art. Again we need a larger sample size to recommend how far back fuels should be removed, but we did observe varnish spalling where burned trees were not directly in front of rock art panels. Fuel reduction near rock art should always be effected by hand tools, since chain saws spew out carbon-rich fumes and flip oil off the chain, adding the potential to contaminate rock art for future dating. Constructing a permanent fire break or fire line, such as a wide sandy path around rock art panels, would also help prevent fire damage in fire prone areas. Managers must often weigh the desire to keep a vegetation screen to reduce visitor damage with the certainty of fire damage in a wildfire. The chalking damage shown in thin sections shows that some research may still be possible despite the chalk. On the other hand, fire has the potential to remove both the varnish data and the petroglyphs themselves if fuels are especially close.

In most cases where managers have not identified massive spalls and other macrodamage on fire-affected petroglyphs, they have assumed that the rock art was not badly damaged and have walked away, doing nothing about the fire-damaged surfaces that will now decay at a rapidly accelerated rate. For most panels at the Whoopup Canyon site, managers would have made this assumption. Microscopy, however, shows extensive damage to the rock varnish and outer rock surfaces, and ash deposits that will accelerate quartz-grain decay and contaminate the glyphs for cation-ratio dating. The damage is a conservation problem that must be taken into consideration in future site management. Probably, most fire-damaged rock art sites fit into this category, in which the full extent of the damage has never been recognized. It is difficult to impossible to protect rock art after a fire starts. In fire-prone areas, we should record the rock art extensively to mitigate future damage. For

some sites, it would be advisable to sample rock coatings if they are appropriate for dating, as part of mitigating against fire.

Acknowledgments: Special thanks to the late James Clark for assistance in electron microscopy. Research was supported by the Bureau of Land Management and in part by sabbatical support from Arizona State University.

REFERENCES

- Allison, R. J. and Bristow, G. E. (1999) The effects of fire on rock weathering: Some further considerations of laboratory experimental simulation. *Earth Surface Processes and Landforms*, Vol. 24, 707–713.
- Allison, R. J. and Goudie, A. S. (1994) The effects of fire on rock weathering: An experimental study, in D. A. Robinson and R. B. G. Williams, eds., *Rock Weathering and Landform Evolution*. Chichester, UK: Wiley, 41–56.
- Blackwelder, E. (1927) Fire as an agent in rock weathering. *Journal of Geology*, Vol. 35, 134–140.
- Brais, S., David, P., and Ouimet, R. (2000) Impacts of wildfire severity and salvage harvesting on the nutrient balance of jack pine and black spruce boreal stands. *Forest Ecology and Management*, Vol. 137, 231–243.
- Carcaillet, C. (1998) A spatially precise study of Holocene fire history, climate and human impact within the Maurienne valley, North French Alps. *Journal of Ecology*, Vol. 86, 384–396.
- Carcaillet, C. and Thion, M. (1996) Pedoanthracological contribution to the study of the evolution of the upper treeline in the Maurienne valley (North French Alps): Methodology and preliminary data. *Review of Palaeobotany and Palynology*, Vol. 91, 399–416.
- Cerda, A. (1998) Relationships between climate and soil hydrological and erosional characteristics along climatic gradients in Mediterranean limestone areas. *Geomorphology*, Vol. 25, 123–134.
- Dixon, J. C., Thorn, C. E., Darmody, R. G., and Campbell, S. W. (2002) Weathering rinds and rock coatings from an Arctic alpine environment, northern Scandinavia. *Geological Society of America Bulletin*, Vol. 114, 226–238.
- Dorn, R. I. (1992) Paleoenvironmental signals in rock varnish on petroglyphs. *American Indian Rock Art*, Vol. 18, 1–17.
- Dorn, R. I. (1995) Digital processing of back-scatter electron imagery: A microscopic approach to quantifying chemical weathering. *Geological Society of America Bulletin*, Vol. 107, 725–741.
- Dorn, R. I. (1998) *Rock Coatings*. Amsterdam, Netherlands: Elsevier.
- Dorn, R. I., (2000), Chronometric techniques: Engravings. In D. S. Whitley, ed., *Handbook of Rock Art Research*. Walnut Creek, CA: AltaMira, 167–189.
- Dorn, R. I. (2003) Boulder weathering and erosion associated with a wildfire, Sierra Ancha Mountains, Arizona. *Geomorphology*, Vol. 55, 155–171.
- Dorn, R. I. and Krinsley, D. H. (1991) Cation-leaching sites in rock varnish. *Geology*, Vol. 19, 1077–1080.
- Dragovich, D. (1993) Fire-accelerated boulder weathering in the Pilbara, Western Australia. *Zeitschrift für Geomorphologie N.F.*, Vol. 37, 295–307.

- Emery, K. O. (1944) Brush fires and rock exfoliation. *American Journal of Science*, Vol. 242, 506–508.
- Frink, D. S. and Dorn, R. I. (2002) Beyond taphonomy: Pedogenic transformations of the archaeological record in monumental earthworks. *Journal of the Arizona-Nevada Academy of Sciences*, Vol. 34, 24–44.
- Garty, J. (1992) The postfire recovery of rock-inhabiting algae, microfungi, and lichens. *Canadian Journal of Botany—Revue Canadienne de Botanique*, Vol. 70, 301–312.
- Germanosky, D. and Miller, J. R. (1995) Geomorphic response to wildfire in an arid watershed, Crow Canyon, Nevada. *Physical Geography*, Vol. 16, 243–256.
- Gordon, S. J. and Dorn, R. I. (in press) In situ weathering rind erosion. *Geomorphology*, Vol. 65.
- Goudie, A. S., Allison, R. J., and McClaren, S. J. (1992) The relations between modulus of elasticity and temperature in the context of the experimental simulation of rock weathering by fire. *Earth Surface Processes and Landforms*, Vol. 17, 605–615.
- Harrison, R. and Frink, D. S. (2000) The OCR carbon dating procedure in Australia: New dates from Wilinyjibari Rockshelter, southeastern Kimberley, Western Australia. *Australian Archaeology*, Vol. 51, 6–15.
- House, J. H. and Smith, J. W. (1975) Experiments in the replication of fire-cracked rock. *Arkansas Archaeological Survey Research Series [The Cache River Archeological Project, assembled by M. B. Shiffer and J. H. House]*, Vol. 8, 75–80.
- Kelly, R. and McCarthy, D. F. (2001) Effects of fire on rock art. *American Indian Rock Art*, Vol. 27, 169–176.
- Krinsley, D. H., Dorn, R. I., and Tovey, N. K. (1995) Nanometer-scale layering in rock varnish: implications for genesis and paleoenvironmental interpretation. *Journal of Geology*, Vol. 103, 106–113.
- Kritzer, K., 1995, Thermolithofractography: A Comparative Analysis of Cracked Rock from an Archaeological Site and Cracked Rock from a Culturally Sterile Area. M.S. Thesis, Anthropology. Master's thesis, Department of Anthropology, Ball State University, Muncie, Indiana.
- Laird, L. D. and Campbell, I. D. (2000) High resolution palaeofire signals from Christina Lake, Alberta: A comparison of the charcoal signals extracted by two different methods. *Palaeogeography, Palaeoclimatology, Palaeoecology*, Vol. 164, 111–123.
- Lichtfouse, E. (1999) Temporal pools of individual organic substances in soil. *Analisis*, Vol. 27, 442–444.
- Lichtfouse, E., Bardoux, G., Mariotti, A., Balesdent, J., Ballentine, D. C., and Macko, S. A. (1997) Molecular, C-13, and C-14 evidence for the allochthonous and ancient origin of C-16-C-18 n-alkanes in modern soils. *Geochimica et Cosmochimica Acta*, Vol. 61, 1891–1898.
- Liu, T. (2003) Blind testing of rock varnish microstratigraphy as a chronometric indicator: results on late Quaternary lava flows in the Mojave Desert, California. *Geomorphology*, Vol. 53, 209–234.
- Mazhitova, G. G. (2000) Pyrogenic dynamics of permafrost-affected soils in the Kolyma Upland. *Eurasian Soil Science*, Vol. 33, 542–551.

- McFarland, P. (1977) Experiments in the firing and breaking of rocks. *Calgary Archaeologist*, Vol. 5, 31–33.
- Morris, S. E. and Moses, T. (1987) Forest-fire and the natural soil-erosion regime in the Colorado Front Range. *Annals of the Association of American Geographers*, Vol. 77, 245–254.
- Nealson, E. (1995) Fire as a Geomorphic Agent in Rock Weathering: The Effect of Rock Size on Weathering Efficiency Under Simulated Forest Fire Conditions. Master's thesis, Department of Geography, University of Iowa, Iowa City, Iowa.
- Ollier, C. D. (1983) Fire and rock breakdown. *Zeitschrift für Geomorphologie*, Vol. 27, 363–374.
- Pentecost, A. (1991) The weathering rates of some sandstone cliffs, central Weald, England. *Earth Surface Processes and Landforms*, Vol. 16, 83–91.
- Pineda, C. A., Peisach, M., Jacobson, L., and Sampson, C. G. (1990) Cation-ratio differences in rock patina on hornfels and chalcedony using thick target PIXE. *Nuclear Instruments and Methods in Physics Research*, Vol. B49, 332–335.
- Plakht, J., Patyk-Kara, N., and Gorelikova, N. (2000) Terrace pediments in Makhtesh Ramon, central Negev, Israel. *Earth Surface Processes and Landforms*, Vol. 25, 29–30.
- Pope, G. A. (1995) Newly discovered submicron-scale weathering in quartz: Geographical implications. *Professional Geographer*, Vol. 47, 375–387.
- Pope, G. A. (2000) Weathering of petroglyphs: Direct assessment and implications for dating methods. *Antiquity*, Vol. 74, 833–843.
- Pope, G. A., Meierding, T. C., and Paradise, T. R. (2002) Geomorphology's role in the study of weathering of cultural stone. *Geomorphology*, Vol. 47, 211–225.
- Prosser, I. P. and Williams, L. (1998) The effect of wildfire on runoff and erosion in native Eucalyptus forest. *Hydrological Processes*, Vol. 12, 251–265.
- Rapp, G. J., Balescu, S., and Lamothe, M. (1999) The identification of granitic fire-cracked rocks using luminescence of alkali feldspars. *American Antiquity*, Vol. 64, 71–78.
- Reed, S. J. B. (1993) *Electron Microprobe Analysis*. (2nd edition). Cambridge, UK: Cambridge University Press, 326.
- Siffedine, A., Bertrand, P., Fournier, M., Martin, L., Servant, M., Soubies, F., Suguio, K., and Turcq, B. (1994) The lacustrine organic sedimentation in tropical humid environment (Carajas, eastern Amazonia, Brazil)—Relationship with climatic changes during the last 60,000 years BP. *Bulletin de la Societe Geologique de France*, Vol. 165, 613–621.
- Thorn, C. E., Darmody, R. G., Dixon, J. C., and Schlyter, P. (2001) The chemical weathering regime of Karkevage, arctic-alpine Sweden. *Geomorphology*, Vol. 41, 37–52.
- Tratebas, A. M. (1993) Stylistic chronology versus absolute dates for early hunting style rock art on the North American Plains. In M. Lorblanchet and P. Bahn, eds., *Rock Art Studies: The Post-Stylistic Era*. Oxford, UK: Oxbow, 163–177.
- Tratebas, A. M. (2000) Evidence of Paleo-Indian and Archaic hunting techniques. *American Indian Rock Art*, Vol. 24, 65–75.
- Viles, H. (1995) Ecological perspectives on rock surface weathering: towards a conceptual model. *Geomorphology*, Vol. 13, 21–35.

- Viles, H. A. (2001) Scale issues in weathering studies. *Geomorphology*, Vol. 41, 61–72.
- Whitley, D. S. and Annegarn, H. J. (1994) Cation-ratio dating of rock engravings from Klipfontein, Northern Cape Province, South Africa. In T. A. Dowson and J. D. Lewis-Williams, eds., *Contested Images: Diversity in Southern African Rock Art Research*. Johannesburg, South Africa: University of the Witwatersrand Press, 189–197.
- Wilson, D. C. (1999) The experimental reduction of rock in a Camas Oven: Towards an understanding of the behavioral significance of fire-cracked rock. *Archaeology in Washington*, Vol. 7, 81–89.
- Zhang, Y., Liu, T., and Li, S. (1990) Establishment of a cation-leaching curve of rock varnish and its application to the boundary region of Gansu and Xinjiang, western China. *Seismology and Geology (Beijing)*, Vol. 12, 251–261.
- Zimmerman, S. G., Evenson, E. B., Gosse, J. C., and Erskine, C. P. (1994) Extensive boulder erosion resulting from a range fire on the type-Pinedale moraines, Fremont Lake, Wyoming. *Quaternary Research*, Vol. 42, 255–265.